Received: 17 November 2022 | Revised: 13 July 2023 | Accepted: 23 July 2023

DOI: 10.1002/wer.10915

RESEARCH ARTICLE

water
ENVIRONMENT RESEARCH

Removal efficiency and energy consumption optimization for carbamazepine degradation in wastewater by electrohydraulic discharge

E. Gwanzura[1] | **D. Ramjugernath**[1] | **S. A. Iwarere**[1,2]

[1]Discipline of Chemical Engineering, School of Engineering, University of KwaZulu-Natal, Durban, South Africa

[2]Department of Chemical Engineering, Faculty of Engineering, Built Environment and Information Technology, University of Pretoria, Pretoria, South Africa

Correspondence
S. A. Iwarere, Department of Chemical Engineering, Faculty of Engineering, Built Environment and Information Technology, University of Pretoria, Hatfield 0028, Pretoria, South Africa.
Email: samuel.iwarere@up.ac.za

Funding information
Water Research Commission, Grant/Award Number: K5/2774/3

Abstract

Objective: The treatment of recalcitrant emerging pollutants is a major concern in wastewater treatment. The purpose of this study was the optimization of emerging recalcitrant pollutant degradation using carbamazepine as a representative pollutant. Investigations of the carbamazepine degradation in wastewater was carried out by manipulating discharge current, air flow rate, and initial concentration to maximize removal efficiency and minimize energy consumption.

Method: The study utilized a three-factor at two levels factorial design with randomized central runs. Discharge current, air flow rate, and initial concentration were the independent variables while to maximize removal efficiency and minimize energy consumption were the response variables. Analysis of variance (ANOVA) was performed on the data.

Results: Discharge current, air flow rate, and initial concentration significantly impacted the removal efficiency to different degrees. However, for energy consumption, only current and air flow rate were the significant variables. The highest removal efficiency obtained was 93% ± 4% for 10 and 40 mg/L initial carbamazepine concentration after 10 min of plasma treatment at a current of 0.45 A and no air flow rate.

Conclusion: The plasma reactor demonstrated the capability to treat high cyclic organic chemical contaminant concentration in wastewater with possible applications in preconcentrated wastewater remediation. However, there is still room for reactor design optimization. One key area of focus is reducing treatment cost, which may be achieved theoretically, pending further experimental investigation, by introducing an alternating current power supply, which can reduce energy consumption by 50%–60%.

Practitioner Points

- Discharge current, air flow rate, and initial concentration all influenced the removal efficiency of carbamazepine.
- For energy consumption, only current and air flow rate were significant variables.
- Higher currents result in an improved highly reactive species and UV generation.
- Treatment cost per m3 for the plasma reactor is higher than established technologies.
- The plasma reactor in the study still requires significant optimization.

KEYWORDS

carbamazepine, degradation, electrical discharge, nonthermal plasma, optimization

INTRODUCTION

Carbamazepine is an important oral psychotropic anticonvulsant pharmaceutical designed and utilized to reduce/prevent abnormal electrical activity in the human brain (Beydoun et al., 2020). Carbamazepine is used alone or in conjunction with other drugs to manage certain kinds of epileptic seizures. Additionally, carbamazepine is used to treat trigeminal neuralgia (a condition that causes facial nerve pain). In individuals with bipolar I illness, carbamazepine is also used to treat manic or mixed episodes (manic-depressive disorder; a disease that causes episodes of depression, episodes of mania, and other abnormal moods) (Maan & Saadabadi, 2021).

The human body cannot fully metabolize carbamazepine, resulting in the drug being expelled unmetabolized in body waste into sewage system. Carbamazepine is a problem pollutant as wastewater treatment plants (WWTP) in their current configuration are unable to treat carbamazepine (Clara et al., 2004; Vieno et al., 2007). Carbamazepine has a stable three-ring phenolic base complex spatial structure that infers its recalcitrant properties. The recalcitrant nature of carbamazepine to wastewater treatment, slow environmental biodegradation results in carbamazepine accumulation in the aquatic environment (Magureanu et al., 2015).

Carbamazepine aquatic accumulation is potentially harmful as uncontrolled intake of carbamazepine may cause life-threatening allergic reactions called Stevens–Johnson syndrome (SJS) or toxic epidermal necrolysis (TEN) and may decrease the number of blood cells produced by the human body (Wanda et al., 2017). Consequently, CBZ can be used as a model polycyclic recalcitrant nonbiodegradable and harmful pollutant as it is frequently found in surface and wastewater (Magureanu et al., 2015).

There has been significant research effort to develop technologies to address CBZ degradation and removal in wastewater, among them reverse osmosis and adsorption (Dwivedi et al., 2017), nonthermal plasma (NTP) (Miklos et al., 2018; Wardenier et al., 2019), and wetlands (Chen et al., 2018). Filtration technology has been very effective in CBZ removal from wastewater (Rodriguez-Mozaz et al., 2015); however, there is the CBZ filtrate disposal problem.

The utilization of NTP technology to complement conventional WWTP might be a viable solution for treating emerging recalcitrant chemical pollutants in wastewater, especially in the tertiary treatment stage. Additionally, NTP wastewater treatment systems can operate economically for concentrated wastewater streams if optimized (Krause et al., 2011).

In the context of wastewater treatment, plasma is generated by strong electric fields between electrodes, which initiate electrical discharges in the water (direct/electrohydraulic discharge) or on the water surface (indirect discharge). The electric discharge produces oxidizing radicals, active species, ultraviolet (UV) radiation, and shockwaves, which degrade chemical pollutants (Jiang et al., 2014).

Different physical and power supply configurations have been implemented for the degradation of CBZ. Previous studies have been effective in the degradation of CBZ, even in very high concentration. However, there has been little work in terms of process optimization to ensure commercial viability. Most studies have used expensive gases (oxygen, nitrogen, and argon) and

utilized reactor configuration and settings, which result in high electricity consumption. There is no information concerning the optimization of multiple factors as well as the interactions of those factors for CBZ degradation using NTP to the best of the authors' knowledge.

In this study, a point-to-plane electrical discharge batch reactor has been developed for the degradation of CBZ at high concentrates in wastewater at atmospheric pressure. The study focuses on two dimensions of wastewater treatment, removal efficiency, and treatment cost as measured by electrical energy consumption.

Removal efficiency and energy consumption can be conceptualized as independent response factors and as related factors, depending on the treatment objective. For a priority pollutant, removal efficiency might take priority over energy consumption and treatment cost. Energy consumption consideration may take precedence when comparing even matched removal efficiencies by different technologies, and the deciding factor comes to the cost of treatment. Removal efficiency and electrical consumption are related; however, they are affected by different factors.

Based on the discussion above, there is a need to optimize NTP treatment technology by identifying the factors influencing removal efficiency and energy consumption and determining factor interactions.

MATERIALS

Distilled water was used in the experiments. CBZ (99.4% purity) was purchased from DLD Scientific, Durban, South Africa (SA), and dichloromethane (DCM) (99% purity) was purchased from Merck., SA. All chemicals were analytical grade and used without further purification.

Experimental setup

This study utilized a point-to-plane electrode configuration inside an electrical discharge batch reactor for the experiment (Figure 1). The electrodes were made of copper rod 8 mm in diameter and spaced at an interelectrode gap of 2 mm. A gap greater than 2 mm resulted in difficulty sustaining the arc discharge as current is continuously pulled from the direct current power supply, while gaps less than 1 mm resulted in excessive electrode wear and melting after extended periods of operation. The assertion that smaller electrode gaps give more satisfactory results is also reported by Fahmy et al. (2020) in dye decoloration optimization studies. The total reactor volume was 500 mL but kept at an operating volume of 300 mL. Synthetic air from a cylinder was used as the feed gas; the air flow rate was regulated with a range of 0–3 L/min selected as the operating range; higher air flow rates disrupted arc stability and could force water to come out at the reactor opening at the top of the reactor as the reactor was operating at atmospheric pressure.

The Technix SR10-R-5000 high voltage power supply supplied direct current (DC) with a voltage range of 0 to 10 kV and a current range of 0 to 0.5 A. The electrodes were connected to the DC power supply in negative polarity as it has a higher voltage gradient than positive

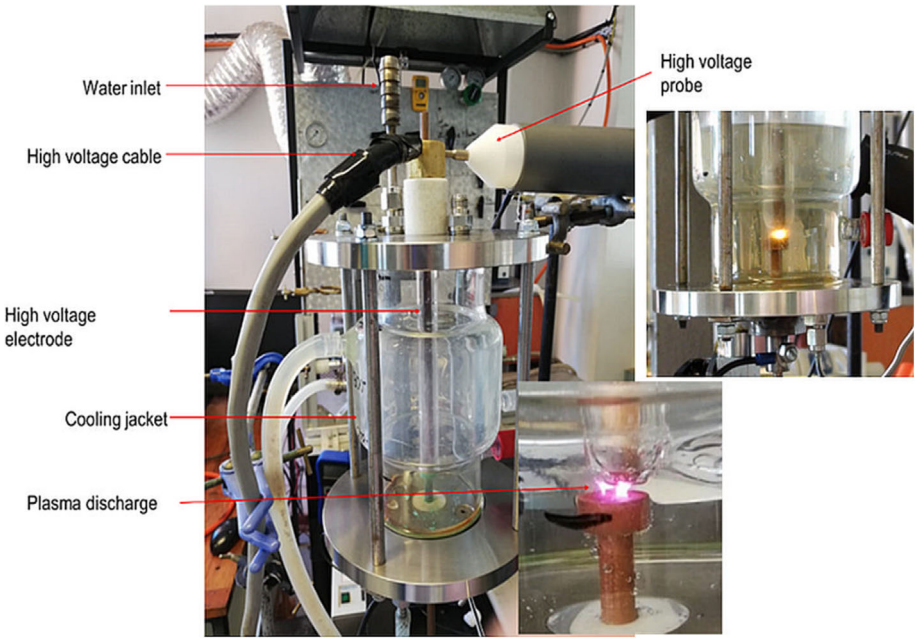

FIGURE 1 Stable electric discharge in 40 mg/L CBZ spiked synthetic wastewater at 2-mm electrode gap, 0.45 A, and 0 L/min.

polarity, although it limits the electrode gap to less than 5 mm. The operating current was set on the high voltage power supply, while the discharge voltage was measured by an Elditest high voltage probe (GMW GmbH & Co. KG, Cadlolzburg, Germany), which is connected to a 500-MHz, four-channel LeCroy WaveJet 354A digital oscilloscope purchased from Lecroy, Japan. The reactor was operated in a semibatch mode with samples taken at 2.5-min intervals.

Sample preparation and analysis

The calibration stock solution of CBZ was prepared to 100 mg/L concentration in DCM in a 100-mL flask (the stock solution was stored at 4°C when not in use). The working calibration solutions (1, 2, 3, 4, 5, 10, 20, 30, 40, and 50 mg/L) of CBZ concentrations were prepared by serial dilution of the stock solution. The quality control (QC) solutions of 1.5, 15, and 35 mg/L were also prepared by serial dilution of the stock solution.

All quantitative analysis was done by GC-2010 Shimadzu Gas Chromatograph-Flame Ionisation Detector (GC-FID) bought at Shimadzu South Africa. All work with GC-FID involved 5-μL manual injection. The separation of the components in the injected sample was achieved using ZB-5MS capillary column (30 m × 0.3 mm × 25 μm). The split mode (5:1) was used with nitrogen carrier gas at 2 mL/min flow rate. Hydrogen and synthetic air were used as auxiliary gases for the detector (FID). The injector port and detector temperatures were set at 270°C. Table S1 in the Supporting Information details the GC-FID oven program. The GC-FID program was optimized for short run time.

Table S2 as presented in Supporting Information shows the key results of the linear regression of the calibration procedure and data for the gas chromatography measurements.

To prepare either a 10, 20, or 40 mg/L of CBZ spiked synthetic wastewater, 5, 10, or 20 mg of CBZ were weighed, respectively, on an analytical balance, measuring in grams up to four decimal places. The weighed CBZ was added to a 0.5-L flask half-filled with distilled water. The flask was shaken to homogenize and filled up to the mark, then allowed to equilibrate.

Water sample preparation for GC analysis involved liquid–liquid extraction (LLE) of a 5-mL water sample in two steps of 1.5-mL dichloromethane per extraction step. After adding the DCM to the water, it was adequately shaken for 5 min and settled for 10 min in a separating funnel. After extraction, the organic phase was removed and transferred into the GC vial and analyzed using GC-FID for quantitative and an Agilent 5977B gas chromatograph/mass spectrometer (GC/MS) for qualitative purposes.

The percentage recoveries in this study are detailed Table S3 as calculated using standard approach from literature (Wardenier, 2016). Literature shows the acceptable range for the recovery of CBZ in the water at 80%–120% (Böger et al., 2018; Krause et al., 2011; Miao & Metcalfe, 2003).

As part of the quality assurance and to ensure consistency, quality control (QC) sample of 1, 20 and 35 mg/L CBZ were randomly injected during the course of analysis. The concentrations of the quality samples were chosen to ensure coverage of the 1–40 mg/L, which was the working range of the experiments. Tables S4 and S5 in the Supporting Information illustrate the intraday and interday variations of the analytical method using QC samples.

Statistical method

The study utilized a factorial design with three (3) factors at two levels for the theoretical examination of the experimental space. The factorial design can be utilized on the basis that the model generated is statistically adequate and allows the screening of factors and interactions which affect the responses (Rakić et al., 2014).

Central points were incorporated in the design at random intervals in the design to provide estimation of pure error and curvature. Additionally, the center points permit the user to check the goodness-of-fit of the planar two-level factorial model.

The central point experimental runs were conducted in triplicates, while noncenter points were conducted in duplicate to measure repeatability. The key performance criteria/response factors are contaminant removal efficiency (Y_1) and energy consumption (Y_2).

The key factors affecting the response factors are the discharge current (current) (A), gas flow rate (flow rate) (B), and initial contaminant concentration (concentration) (C) as they have been identified as the three most critical independent parameters.

Each independent factor with two different levels, which are coded as −1 (low) and +1 (high), center points are designated as (0) as shown in Table 1.

Running the full complement of all possible factor combinations means that the main and interaction effects can be estimated. There are three main effects, 3 two-factor interactions and a three-factor interaction, all of which appear in the full model as shown in Equation (1).

TABLE 1 Design factors and their level values.

Factor	Code	Low (−1)	Centre point (0)	High (1)	Unit
Current	A	0.250	0.350	0.450	A
Flow rate	B	0	1	3	L/min
Concentration	C	10	20	40	mg/L

TABLE 2 Experimental values of removal efficiency and energy consumption at design values.

Run	Factor 1 A: Current (A)	Factor 2 B: Flow rate (L/min)	Factor 3 C: Concentration (mg/L)	Response 1 Removal efficiency (%)	Response 2 Energy consumption (kWh)
1	−1	−1	−1	73.13	0.0049
2	−1	−1	1	34.27	0.0051
3	1	1	−1	46.95	0.0155
4	−1	−1	1	34.78	0.0049
5	1	−1	−1	90.04	0.0152
6	1	−1	1	94.96	0.0149
7	−1	1	−1	42.81	0.0054
8	−1	1	1	42.57	0.0052
9	0	0	0	58.59	0.0123
10	0	0	0	59.96	0.0121
11	1	−1	1	96.84	0.0152
12	−1	−1	−1	74.54	0.0151
13	1	1	1	69.13	0.0156
14	1	−1	−1	89.50	0.0151
15	0	0	0	60.59	0.0120
16	1	1	1	70.55	0.0157
17	1	1	−1	48.43	0.0153
18	−1	1	−1	42.83	0.0051
19	−1	1	1	42.48	0.0056

Note: Energy consumption is for the treatment of 300 mL, the operational capacity of the reactor.

$$\text{Response factor (Y)} = C_0 + C_1A + C_2B + C_3C + C_4AB + C_5AC + C_6BC + \varepsilon \quad (1)$$

The terminologies C_i are constants and ε is an error term,

A factorial design with a minimum resolution of 5 allows for the estimation of all the eight-factor coefficients (however, three-factor interactions are ignored as they are insignificant for categorical factors). Factorial models in Design Expert® Software Version 7.0 do not produce polynomials, thus excluding curvature from the lack-of-fit test and the residuals, and providing more precise information about the fit of the model (the software does a separate test for the curvature). One benefit of this procedure is that the assumptions concerning normality and constant variance can be checked even in the presence of curvature. This allows for the identification of any problems in the data analysis that might otherwise be obscured by curvature inflating the residuals. Table 2 depicts the full list of random experimental runs.

RESULTS AND DISCUSSION

The effect of the plasma treatment on water quality, namely, pH and conductivity, warrant a brief discussion.

Irrespective of the starting concentration and operating conditions, there was a general decrease in the pH of all the plasma-treated CBZ wastewater from the initial pH of 7.3. Different operational conditions produced different final pH values. A current of 0.45 A and air flow rate of 3 L/min resulted in the highest pH drop after plasma treatment resulting in an average final pH value of 2.9. A current of 0.25 A and air flow rate of 0 L/min resulted in the smallest pH drop after plasma treatment

resulting in an average final pH value of 3.7. Literature suggests that acidification of plasma-treated water is the result of nitrous acid (HNO_2) and nitric acid (HNO_3) formation in the bulk liquid (Kogelschatz et al., 2003). The formation of nitrite and nitrate also results in the production of hydrogen cations (H^+) in the aqueous phase, which describes the experimentally observed pH drop by plasma discharges in air (Lukes et al., 2012). The contribution of nitrogen compounds to reduced pH is justified by the fact that the lowest pH recorded (2.9) was under 3 L/min air flow, air that contains approximately 78% nitrogen, which acts as an additional supply of nitrogen into the water hence driving reactions reducing pH. However, significant pH drops have also been reported in literature in solutions treated in nitrogen-free plasmas. For instance, a final pH value of 2.07 after oxygen DBD plasma treatment of deionized water has been reported (Shainsky et al., 2012). This suggests that other reactive species, formed in the liquid phase, contribute as well to the acidification of deionized water in the plasma chamber. Probably, the self-decomposition of ozone, produced in the plasma discharge, contributes to significant lower pH values.

In addition to the pH measurements, also changes in solution conductivity were measured. The initial conductivity was 0.24 ± 0.06 μS/cm. The general trend is an increase in the initial conductivity due to plasma treatment. The final conductivity is a function of the discharge current and the air flow rate. The highest final conductivity was that of water treated at the highest current (0.45 A) and air flow rate (3 L/min), which produced a final conductivity of 439 μS/cm. Air appears to be the dominant contributor to the conductivity as the conductivity for 0.45 A and 0 L/min is close to the conductivity of 0.25 A and 3 L/min. The role of air flow rate in influencing conductivity may be attributed to how air flow rate at 3 L/min resulted in discharge instability hence more marked electrode degradation, thus depositing more copper ions in the solution which contributes to an increase in conductivity since 0.25 A and 3 L/min has conductivity almost equal to 0.45 A and 0 L/min.

Model analysis

The total number of runs was 19, including the three (3) replicates using the center points' processing parameters. The model is a factorial model with a maximum of two-factor interactions. Table 2 shows the experimental runs and the values for the removal efficiency and energy consumption for all the 19 experimental runs.

The model evaluation revealed that the lack of fit and pure error had 4 degrees of freedom (df) and 10 df, respectively. This is acceptable as the Design Expert® Software Version 7.0 recommendation is a minimum of 3 lack of fit df and 4 df for pure error to perform a valid lack of fit test for the generated model.

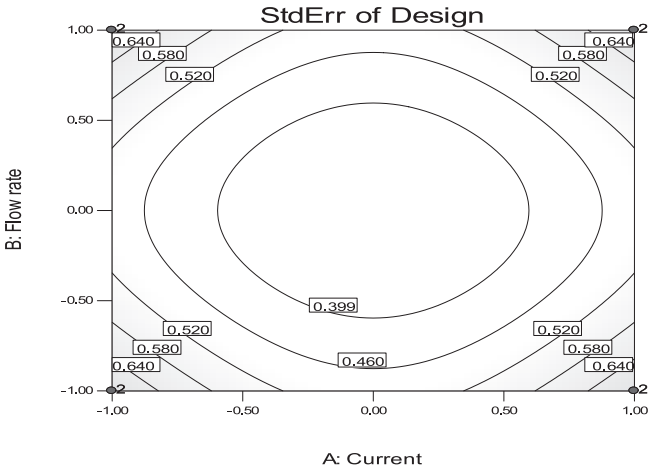

FIGURE 2 Design evaluation graph for standard error at 10 mg/L with the design pints marked in red at the corners of the plot.

Figure 2 shows the standard error of prediction for areas in the design space at 10 mg/L CBZ. The standard error must be low, approximately 1.0 or lower. Figure 2 shows a maximum standard error across the region of interest of 0.64, which is acceptable. The design evaluation graph for +1 level of concentration (40 mg/L) also show a maximum standard error of 0.64.

The ANOVA analysis was performed to determine the regression models' significance and adequacy for both removal efficiency and energy consumption as represented by Figure 3. For both responses, no transform was assigned as the ratio of the maximum, and the minimum was less than 10, specifically 2.82 for removal efficiency and 3.2 for energy consumption. ANOVA showed that the models were significant and had F values of 1407.29 and 2056.93 for removal efficiency (Table 3) and energy consumption (Table 4), respectively. The values of the respective R^2 values are comparable. Additionally, the adequate precision that measures the signal-to-noise are above the recommended minimum of 4. The conclusion from the ANOVA is that this model can be used to navigate the design space.

Equations (2) and (3) are determined by ANOVA as the equations that describe the relationship between the response factors and the significant independent variable.

$$Energy\ consumption = 0.010 + (0.005075 * Current) + (0.0001855 * flowrate) \quad (2)$$

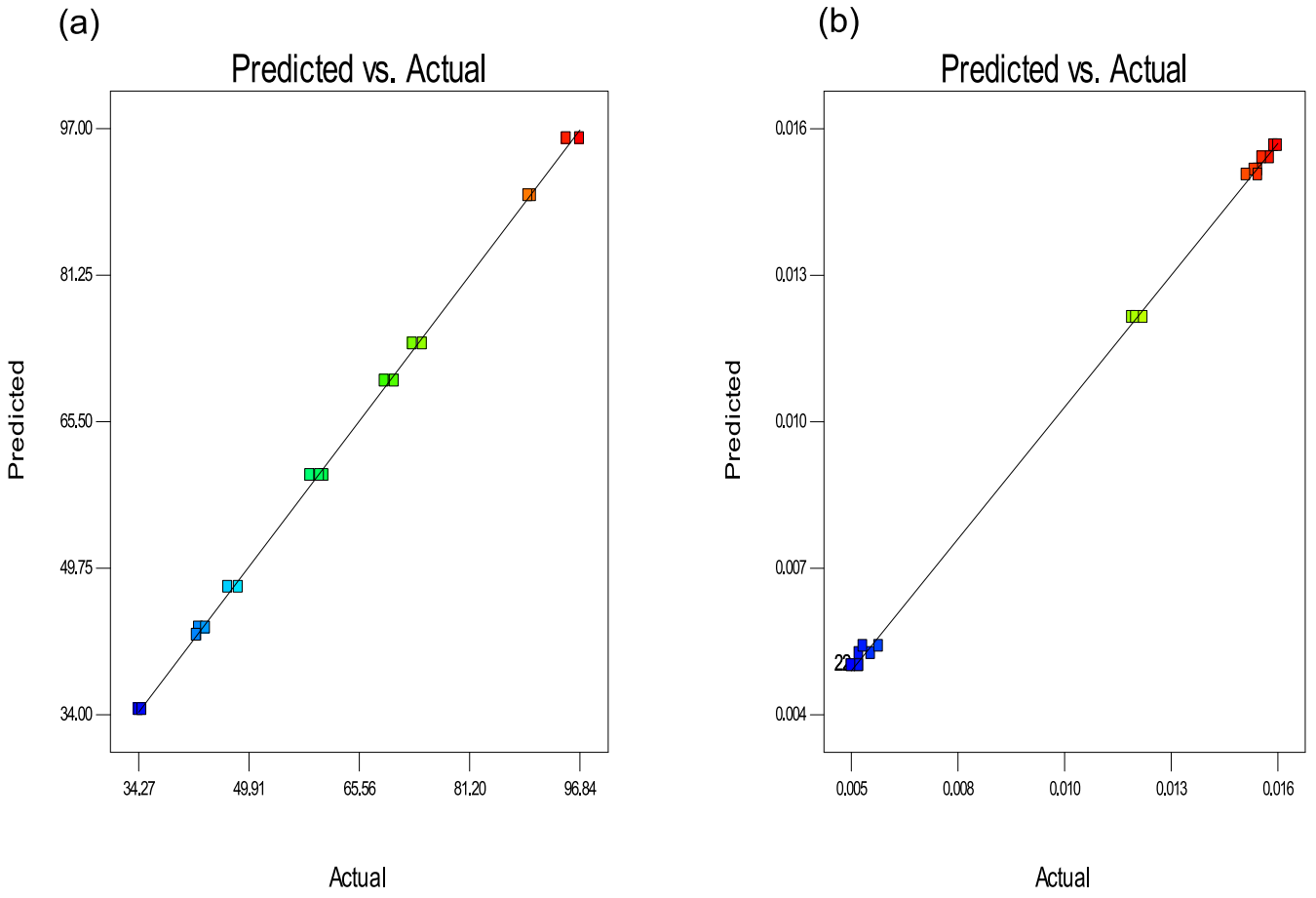

FIGURE 3 Experimental versus predicted results (a) removal efficiency; (b) energy consumption.

TABLE 3 Results of ANOVA for the factorial model for the removal efficiency.

Source	Sum of squares	Df	Mean square	*F* value	*p* value Prob > F	Comment
Model	7620.59	7	1088.66	1407.29	<0.0001	Significant
A—Current	2971.07	1	2971.07	3840.66	<0.0001	
B—Flow rate	2055.49	1	2055.49	2657.11	<0.0001	
C—Concentration	34.84	1	34.84	45.04	<0.0001	
AB	519.95	1	519.958	672.14	<0.0001	
AC	1198.44	1	1168.44	1510.43	<0.0001	
BC	744.06	1	744.06	961.84	<0.0001	
ABC	126.73		12.73	163.82		
Curvature	15.29	1	15.29	19.76	0.0012	Significant
Pure error	7.74	10	0.77			
Cor Total	7643.61	18				

Note: R^2 0.9990; adjusted R^2 0.9983; predicted R^2 0.9964; adequate precision 101.39.

TABLE 4 Results of ANOVA for the factorial model of the energy consumption.

Source	Sum of squares	Df	Mean square	*F* value	*p* value Prob > F	Comment
Model	4.128E−004	7	5.897E−005	2056.93	<0.0001	Significant
A—Current	4.121E−004	1	4.121E−004	14375.23	<0.0001	
B—Flow rate	5.625E−007	1	5.625E−007	19.62	0.0013	
C—Concentration	2.250E−008	1	2.250E−008	0.78	0.3965	
AB	1.000E−008	1	1.000E−008	0.35	0.5679	
AC	0.000	1	0.000	0.000	1.000	
BC	6.250E−008	1	6.250E−008	2.18	0.1706	
ABC	1.000E−008	1	1.000E−008	0.35	0.5679	
Curvature	9.080E−006	1	9.080E−006	316.75	<0.0001	Significant
Pure error	2.867E−007	10	2.867E−008			
Cor Total	4.221E−004	18				

Note: R^2 0.9993; adjusted R^2 0.9988; predicted R^2 0.9978; adequate precision 91.394.

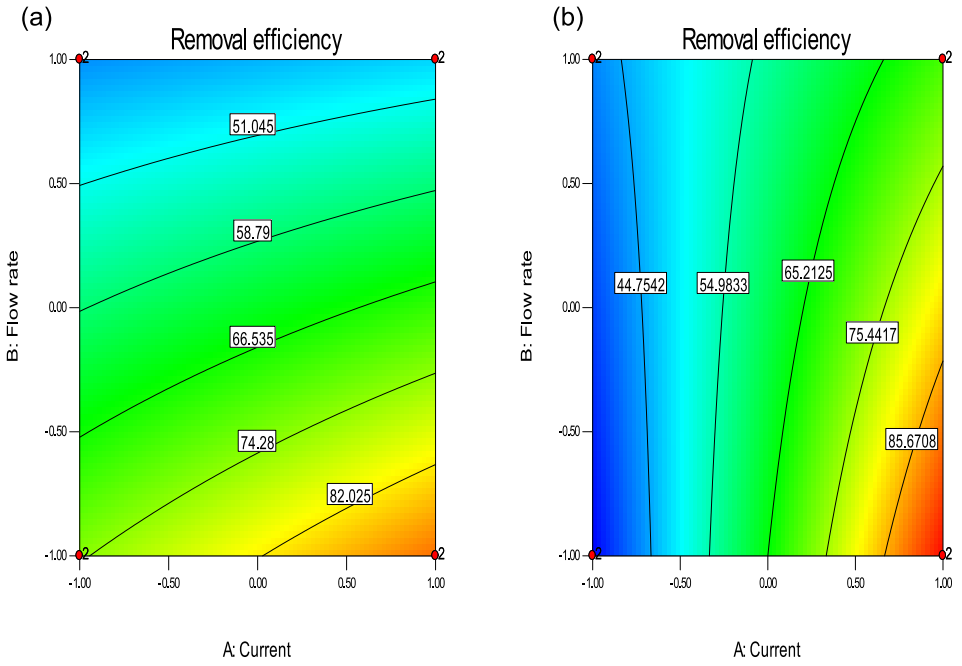

FIGURE 4 Effect of current and flow rate and their interaction on removal efficiency at (a) 10 mg/L; (b) 40 mg/L (contour lines show removal efficiency).

$$\begin{aligned} \textit{Removal efficiency} = {} & 62.17 + (13.63 * \textit{Current}) \\ & - (11.33 * \textit{Flow rate}) \\ & - (1.48 * \textit{Concentration}) \\ & - (5.7 * \textit{Current} * \textit{Flowrate}) \\ & + (8.55 * \textit{Current} * \textit{Concentration}) \\ & - (6.82 \\ & * \textit{Flow rate} * \textit{Concentration}) \\ & + (2.84 * \text{Current} * \text{Flow rate} * \text{Concentration}) \end{aligned} \quad (3)$$

Figure 3a,b shows the comparison between the predicted values from the model generated by Equations (2) and (3) against the actual experimental values.

Effect of process parameters on removal efficiency

The process parameters or interactions with *p* values below the critical value of 0.05 are considered to have a significant impact on the removal efficiency (refer to

Table 4). Current, flow rate, concentration, current-flow rate interaction, current–concentration interaction, and the flow rate–concentration interaction are the significant terms. Among the significant terms, the current, flow rate, and current–concentration interaction are the most significant as they have the largest *F* value. The current and the current-flow rate–concentration interaction are the least significant terms as they have the smallest *F* (refer to Table 4). The effects of process parameters and their interactions in influencing CBZ degradation are presented in Figures 5–7. The discussion will focus on the effect of the two-factor interactions on removal efficiency. The effect of one factor, for example, current on removal efficiency does not give much information as it would just determine if the factor and removal efficiency have a positive or negative relationship; this relationship is depicted in Equations (2) and (3).

Figure 4a,b shows the effects of the current and flow rate on CBZ degradation at concentrations of 10 and 40 mg/L, respectively.

Irrespective of the starting concentration, an increase on current increases removal efficiency while an increase in air flow rate up to values less than 1 L/min increase the removal efficiency. Increasing the air flow rate above 1 L/min starts to reduce the removal efficiency. The current–flow rate interaction for the 10–40 mg/L has a maximum removal efficiency of 82%–85%. Lower flow rates appear to favor enhanced removal efficiency for 10 mg/L starting concentration across the whole current range according to Figure 4a. Figure 4b suggests that the effect of the air on removal efficiency for 40 mg/L is minimal as the contours are almost vertical (small angle to the horizontal); the effect of air increases slightly as the current increases past 0.35 A.

According to Figure 5, lower flow rate results in higher removal efficiency irrespective of the starting concentration or current result. The highest removal efficiency at 0 L/min is 85.67% (Figure 5a) as compared with the highest removal efficiency of 65.29% at 3 L/min. Figure 5a shows that at 0 L/min, as the current nears 0.45 A, removal efficiency becomes independent of the initial concentration. Flow rate of 3 L/min causes an interaction of the current and concentration for any current or concentration range. Lower flow rates may be beneficial as they improve the mass transfer of the reactive species from the gas phase to the liquid phase. Additionally, the introduction of air, while it is beneficial in terms of adding oxygen and enhancing the radical

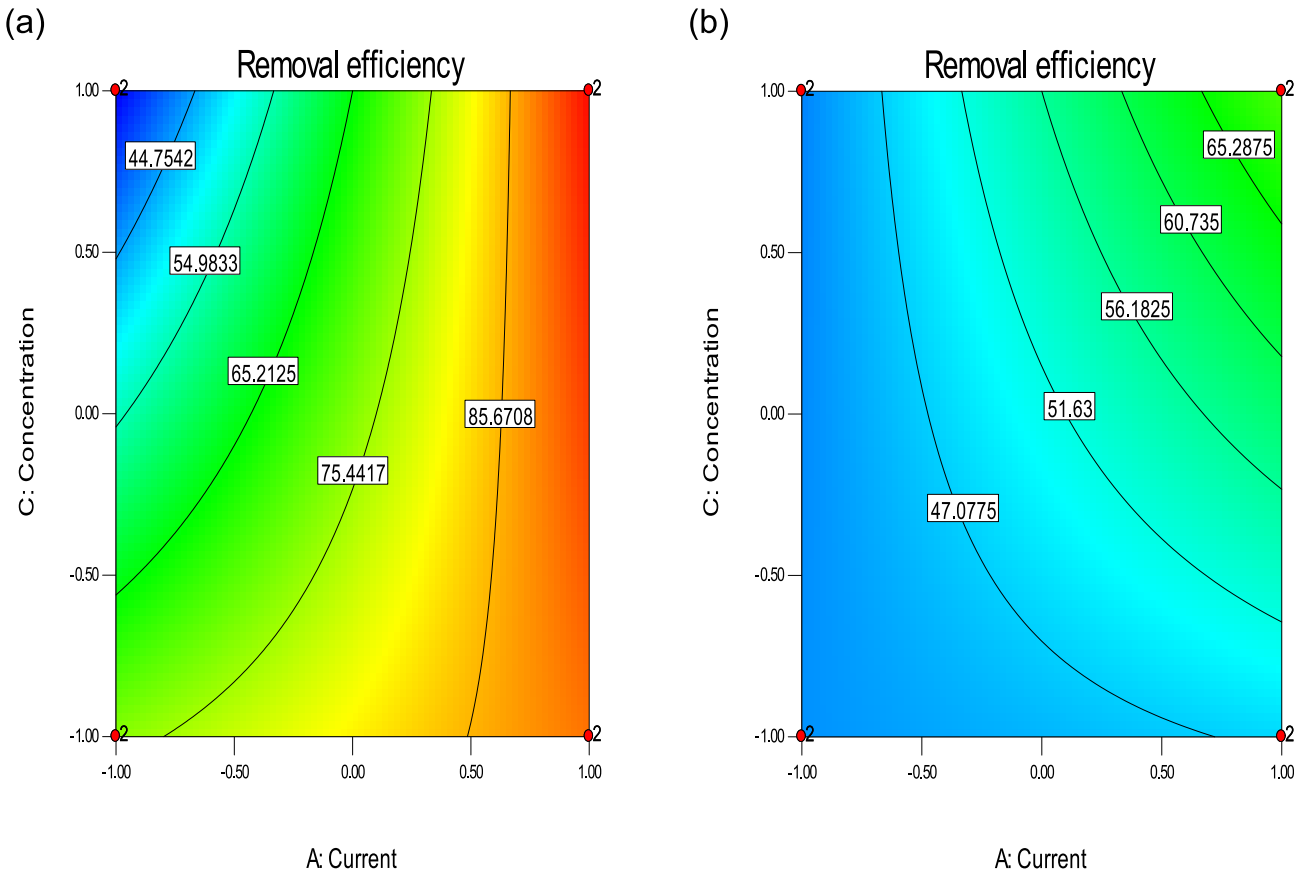

FIGURE 5 The effect of current–concentration interaction on removal efficiency at (a) 0 L/min and (b) 3 L/min (contour lines show removal efficiency).

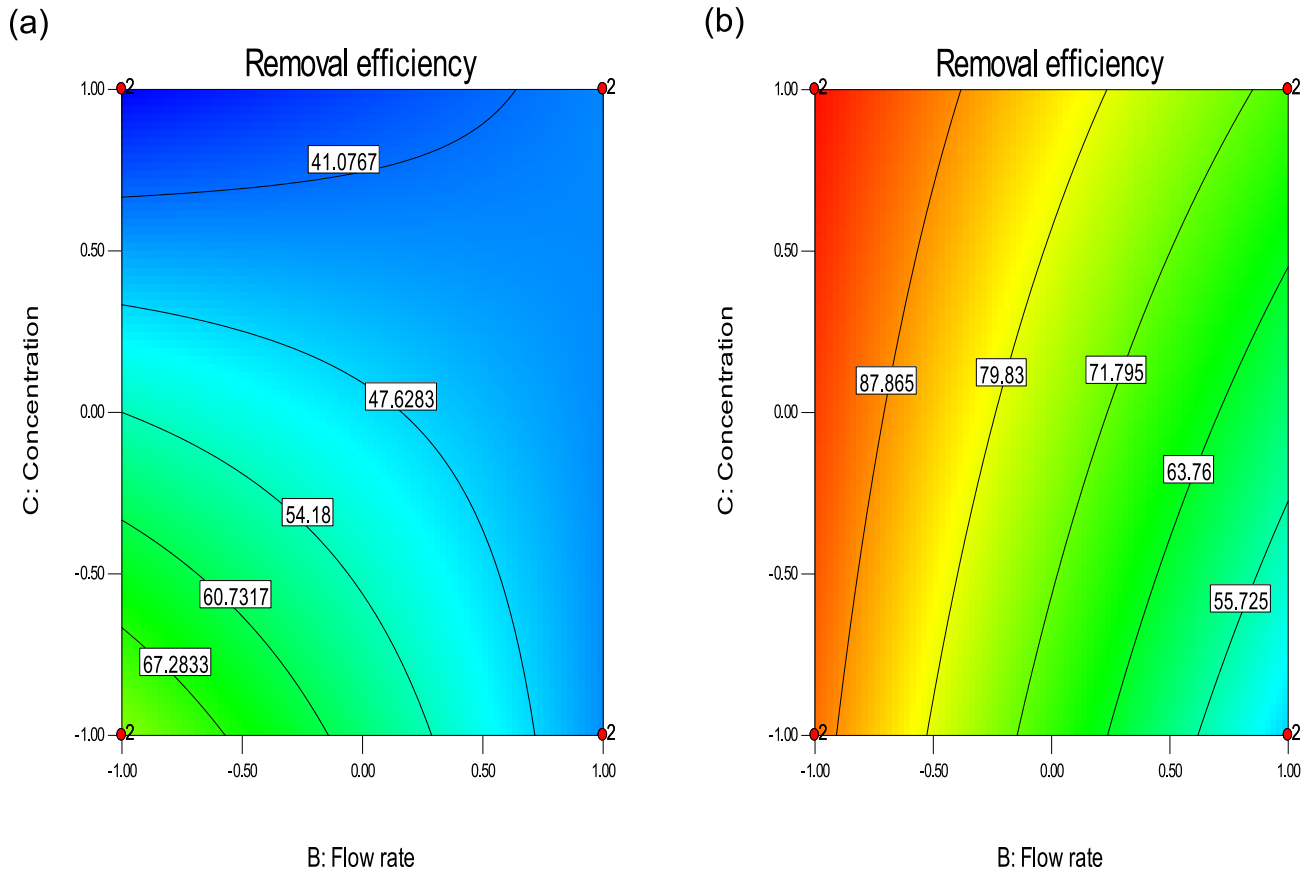

FIGURE 6 Effect of flow rate and concentration and their interaction on removal efficiency at (a) 0.25 A and (b) 0.45 A (contour lines show removal efficiency).

formation, has a negative side effect of disrupting arc stability due to the formation of bubbles and stirring the water.

Figure 6 shows that an increase in the flow rate and initial concentration reduces the removal efficiency individually or together. The effect of the flow rate and initial concentration on removal efficiency is more marked for lower current setting (Figure 6a).

Effect of process parameters on energy consumption

The ANOVA results show the effect of the individual process parameters and *p* values on energy consumption (see Table 4). The current and flow rate are significant factors as their *p* values are below the critical value of 0.05. The current is the dominant factor affecting the energy efficiency of the plasma process with the highest *F* value and lowest *p* value. The discussion will only focus on the current and flow rate as they are the only two factors involved, and there are no interactions.

Figure 7 shows the direct relationship between the energy consumption and the current irrespective of the initial CBZ concentration or flow rate setting (the black line signifies air flow rate at 0 L/min and the red line shows the air flow rate 3 L/min).

While increasing the air flow rate does result in increased energy consumption (the red line above the black line), the difference is minimal as the two lines are close together. The insignificance of the starting concentration for the 10–40 mg/L range is in agreement with the assertion that at initial starting concentrations below 100 mg/L, E_{EO} values are not affected by initial concentration (Bolton et al., 1996).

In Figure 7, the current and energy consumption graph shows a straight line with a positive gradient at an approximately 45° angle for all current and flow rate variations and combinations. The observation is logical for direct current (DC) as the power supply source, and, eventually, energy consumption is directly proportional to the current.

The increase in energy consumption due to the increased air flow rate may be due to the noted discharge instability at a higher air flow rate. Discharge instability

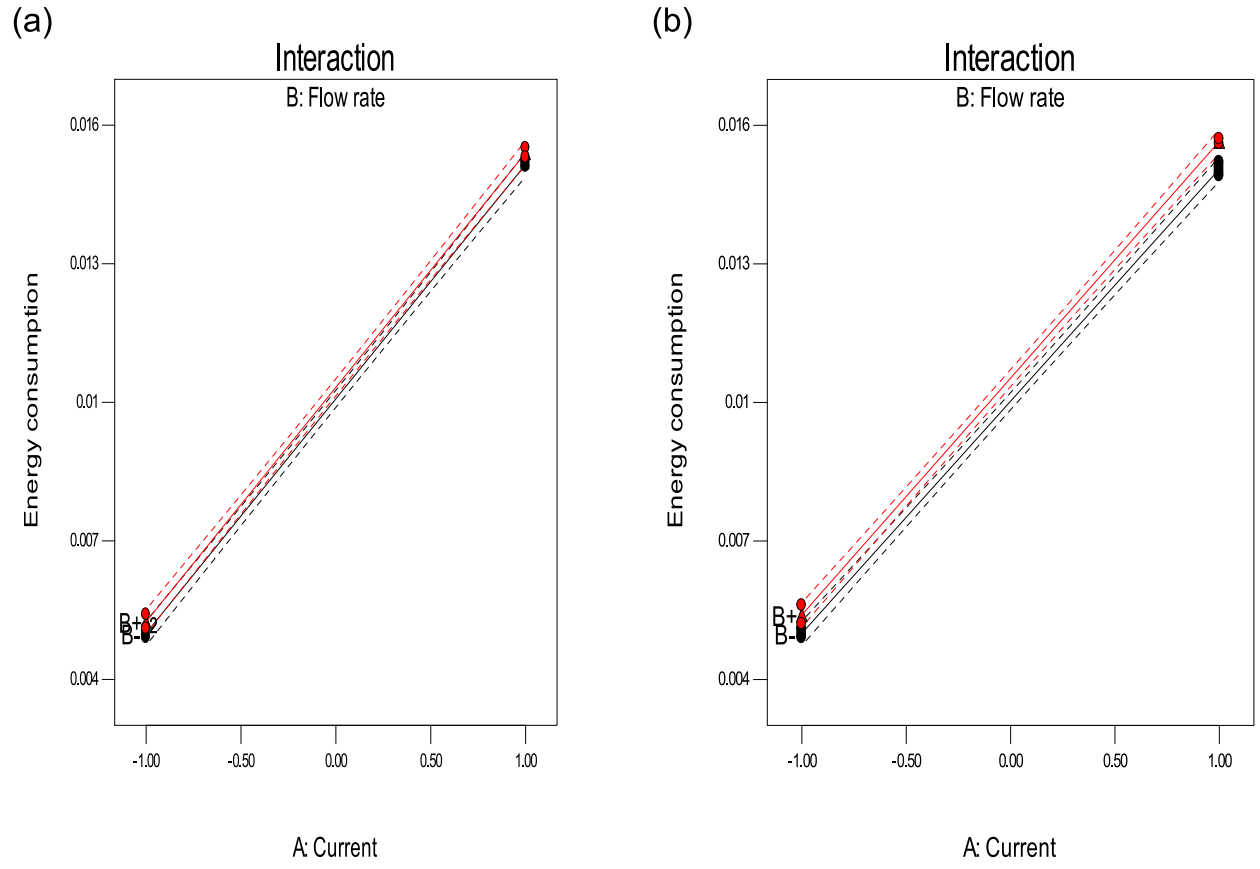

FIGURE 7 The effect of current and flow rate at (a) 10 mg/L and (b) 40 mg/L showing no interactions as demonstrated by the parallel red line and black lines.

TABLE 5 Optimization constraints for economical operation.

Constraint	Goal	Lower limit	Upper limit
Current	In range	−1	1
Flow rate	Minimize	−1	1
Concentration	Maximize	−1	1
Removal efficiency	Maximize	33.9	99
Electricity consumption	Minimize	0.005	0.015

results in an increase in voltage as electric discharge ignition requires higher voltages (breakdown voltage) as compared with maintaining the discharge.

Constraint bound optimization

Optimization in this study is aimed at cost reduction as the process has very high operating costs. The most economic treatment involves reducing process costs (energy consumption and air flow rate and having the highest removal efficiency). Cost reduction involves setting the process parameters to the settings in Table 5.

Optimization focus is intuitive as it is trying to maximize output and minimize input. Costs related to the process include electricity, and air, hence, the optimization criteria were to reduce cost. The concentration was aimed at treating the highest CBZ concentration. The goal was to maximize CBZ removal efficiency and minimize electric energy consumption (reduce cost).

Numerical optimization was utilized as it searches the design space, using the models created in the analysis, to find factor settings that meet the defined goals. The set conditions produced 13 solutions (see Table S6 as presented in the Supporting Information for the first five sample solutions of the optimization). Figure S1 in the Supporting Information shows a sample solution and set values for the optimization. It can be concluded that the removal efficiency and energy consumption of the plasma treatment process in this study cannot reach

the desirable values simultaneously, which results in the most economic runs. The set conditions and the outputs calculated had maximum desirability of 0.715. Desirability is an objective function that ranges from zero outside of the limits to one at the goal. The numerical optimization finds a point that maximizes the desirability function (Table S6).

CBZ degradation byproducts

Equally crucial to the removal efficiency are the products of the CBZ degradation process. Ideally, a treatment process should not produce byproducts more harmful than the parent compound. The presented byproducts are for the best removal efficiency with the highest starting concentration (run 6 and 11 in Table 2).

The qualitative analysis utilized an Agilent 5977C GC/MSD instrument to analyze the samples. The separation was achieved using a ZB-5MS capillary column (30 m × 0.3 mm × 25 μm,) with helium as the carrier gas. The MS detector was set in scan mode. The column temperature was set at 80°C with an injection temperature at 250°C using split injection mode.

Table S7 in the Supporting Information shows the oven program for the qualitative analysis using the gas chromatograph mass spectrometer (GC–MS). The pressure was set at 37.2 kPa with a total flow of 4.4 ml/min and a column flow of 0.69 ml/min with a linear velocity of 30.6 cm/sec at purge flow of 3.0 ml/min using a split ratio of 100.0. The ion source temperature was set at 240°C with an interfacial temperature of 280°C and solvent delay time set at 4.00 min to prevent oversaturation of the column and maintain the long lifespan of the column, and detector gain was set at 0.94 kV. The total run time was 20.28 min, and the scan speed was 1428 with m/z range from 35 to 500.

In this study, an initial qualitative characterization of a pure CBZ was done to identify the mass to charge ratio (m/z) of the pure CBZ (Figure S2) as presented in the Supporting Information. To determine the products of the treatment, a mass spectrum of the CBZ after a 10-min treatment at 0.45 A and 0 L/min air which produced the highest removal efficiency was conducted and the results shown in Figure S3.

To identify possible degradation products, a comparison of fragments from the mass spectra of the pure CBZ before degradation against the mass spectra of CBZ degradation by NTP was conducted. CBZ degradation was confirmed as the CBZ identifier m/z fragments were no longer the base ions.

Figure S3 as presented in the Supporting Information show 44, 57, 71, 85, 135, 207 m/z fragments as the major degradation product. In all the qualitative results, a 44 m/z fragment present signifying the breaking of the CHON fragment from the nitrogen on the center ring of CBZ to produce iminostilbene shown in Figure S4. Ring cleavage of the iminostilbene rings is a possible pathway as the final product with a corresponding m/z spectrum (Figure S3) is a two ring Pterin-6-carboxylic acid as shown in Figure S5. Degradation pathway is postulated to start by the breaking of the (HN=C=O) molecule from the CBZ main molecule to form iminostilbene; the CHON molecule is responsible for the straight-chain alkane 44 m/z fragment while the tricyclic remainder of the CBZ molecule attributes for the 193 m/z fragment. Subsequent cleavage of the 193 m/z fragment at either of the bonds joining the six-sided cyclic to the center seven-sided cyclic produces the 57 m/z and a two-ring 135 m/z fragments. Further ring cleavage of the bond joining the seven-sided cyclic to the seven-sided cyclic of the 135 m/z fragments produces another straight-chain alkane 57 m/z fragment and a seven-sided ring 91 m/z fragment. The 91 m/z cyclic fragment is possibly further opened to produce the 85 and 71 m/z fragments. However, a thorough examination of degradation byproducts and reaction pathways was not the focus of this study.

CONCLUSION

This study examines the effects of the key electrohydraulic process parameters (current, air flow rate, and starting concentration) and their interactions on CBZ degradation and electrical energy consumption.

Optimization shows a minimum of 68.92% removal, which is higher than the degradation achieved by most technologies. The optimization constraints calculate the energy consumption of, on average 0.01 kWh/0.3 L, which translates to approximately 33.3 kWh/m^3, a value still above the 5 kWh/m^3 economic viability benchmark EEO for AOPs. A possible avenue for improving efficiency is the utilization of steel electrodes which has been reported to provide better degradation than copper electrodes at identical conditions (Fahmy et al., 2018). Nonetheless, it is important to realize that high energy consumption may be feasible given the high contaminant concentration. The concentrations of CBZ used are in the mg/L and typical of landfill leachate and other extremely concentrated wastewaters compared with ng/L range in other studies.

A future perspective for this study is the use of a high voltage alternating current power supply at frequencies lower than 20 kHz to further reduce the energy consumption. Additionally, a more advised study with carbon 13 atoms as tracers at different carbamazepine ring

positions should be conducted to better understand carbamazepine degradation pathways.

AUTHOR CONTRIBUTIONS

E. Gwanzura: Conceptualization; methodology; validation; formal analysis; investigation; writing—original draft; writing—review and editing. **D. Ramjugernath:** Supervision; funding acquisition; validation; writing—review and editing; resources. **S. A. Iwarere:** Conceptualization; methodology; validation; writing—review and editing; supervision; funding acquisition; project administration; resources.

ACKNOWLEDGMENTS

We would like to acknowledge the Thermodynamics Research Unit in the Discipline of Chemical Engineering at the University of KwaZulu-Natal for availing a laboratory for conducting experimental work. The project was funded by the Water Research Commission Project No: K5/2774/3.

CONFLICT OF INTEREST STATEMENT

The authors declare that they have no competing interests that could have appeared to influence the work reported in this paper.

DATA AVAILABILITY STATEMENT

The authors confirm that the data that support the findings of this study are available in the Supporting Information of this article.

ORCID

S. A. Iwarere https://orcid.org/0000-0001-8566-6773

REFERENCES

Beydoun, A., Dupont, S., Zhou, D., Matta, M., Nagire, V., & Lagae, L. (2020). Current role of carbamazepine and oxcarbazepine in the management of epilepsy. *Seizure*, *83*, 251–263. https://doi.org/10.1016/j.seizure.2020.10.018

Böger, B., Amaral, B. D., Estevão, P. L. D. S., Wagner, R., Peralta-Zamora, P. G., & Gomes, E. C. (2018). Determination of carbamazepine and diazepam by SPE-HPLC-DAD in Belém River water, Curitiba-PR/Brazil. Revista Ambiente & Água, 13.

Bolton, J. R., Bircher, K. G., Tumas, W., & Tolman, C. A. (1996). Figures-of-merit for the technical development and application of advanced oxidation processes. *Journal of Advanced Oxidation Technologies*, *1*, 13–17.

Chen, X., Hu, Z., Zhang, Y., Zhuang, L., Zhang, J., Li, J., & Hu, H. (2018). Removal processes of carbamazepine in constructed wetlands treating secondary effluent: A review. *Water*, *10*, 1351. https://doi.org/10.3390/w10101351

Clara, M., Strenn, B., & Kreuzinger, N. (2004). Carbamazepine as a possible anthropogenic marker in the aquatic environment: Investigations on the behaviour of carbamazepine in wastewater treatment and during groundwater infiltration. *Water Research*, *38*, 947–954. https://doi.org/10.1016/j.watres.2003.10.058

Dwivedi, K., Morone, A., Pratape, V., Chakrabarti, T., & Pandey, R. A. (2017). Carbamazepine and oxcarbazepine removal in pharmaceutical wastewater treatment plant using a mass balance approach: A case study. *Korean Journal of Chemical Engineering*, *34*, 2662–2671. https://doi.org/10.1007/s11814-017-0190-2

Fahmy, A., El-Zomrawy, A., Saeed, A. M., Sayed, A. Z., El-Arab, M. A. E., Shehata, H., & Friedrich, J. (2020). Degradation of organic dye using plasma discharge: Optimization, pH and energy. *Plasma Research Express*, *2*, 015009. https://doi.org/10.1088/2516-1067/ab6703

Fahmy, A., el-Zomrawy, A., Saeed, A. M., Sayed, A. Z., Ezz el-Arab, M. A., & Shehata, H. A. (2018). Modeling and optimizing Acid Orange 142 degradation in aqueous solution by non-thermal plasma. *Chemosphere*, *210*, 102–109. https://doi.org/10.1016/j.chemosphere.2018.06.176

Jiang, B., Zheng, J., Qiu, S., Wu, M., Zhang, Q., Yan, Z., & Xue, Q. (2014). Review on electrical discharge plasma technology for wastewater remediation. *Chemical Engineering Journal*, *236*, 348–368. https://doi.org/10.1016/j.cej.2013.09.090

Kogelschatz, U., Eliasson, B., & Egli, W. (2003). Plasma Chem. Plasma Process.

Krause, H., Schweiger, B., Prinz, E., Kim, J., & Steinfeld, U. (2011). Degradation of persistent pharmaceuticals in aqueous solutions by a positive dielectric barrier discharge treatment. *Journal of Electrostatics*, *69*, 333–338. https://doi.org/10.1016/j.elstat.2011.04.011

Lukes, P., Locke, B. R., & Brisset, J.-L. (2012). Aqueous-phase chemistry of electrical discharge plasma in water and in gas-liquid environments. *Plasma Chemistry and Catalysis in Gases and Liquids*, *1*, 243–308.

Maan, J. S., & Saadabadi, A. (2021). Carbamazepine. *StatPearls [Internet]*. StatPearls Publishing.

Magureanu, M., Mandache, N. B., & Parvulescu, V. I. (2015). Degradation of pharmaceutical compounds in water by non-thermal plasma treatment. *Water Research*, *81*, 124–136. https://doi.org/10.1016/j.watres.2015.05.037

Miao, X.-S., & Metcalfe, C. D. (2003). Determination of carbamazepine and its metabolites in aqueous samples using liquid chromatography−electrospray tandem mass spectrometry. *Analytical Chemistry*, *75*, 3731–3738. https://doi.org/10.1021/ac030082k

Miklos, D. B., Remy, C., Jekel, M., Linden, K. G., Drewes, J. E., & Hubner, U. (2018). Evaluation of advanced oxidation processes for water and wastewater treatment—A critical review. *Water Research*, *139*, 118–131. https://doi.org/10.1016/j.watres.2018.03.042

Rakić, T., Kasagić-Vujanović, I., Jovanović, M., Jančić-Stojanović, B., & Ivanović, D. (2014). Comparison of full factorial design, central composite design, and Box-Behnken design in chromatographic method development for the determination of fluconazole and its impurities. *Analytical Letters*, *47*, 1334–1347. https://doi.org/10.1080/00032719.2013.867503

Rodriguez-Mozaz, S., Ricart, M., Kock-Schulmeyer, M., Guasch, H., Bonnineau, C., Proia, L., De Alda, M. L., Sabater, S., & Barcelo, D. (2015). Pharmaceuticals and pesticides in reclaimed water: Efficiency assessment of a microfiltration-reverse

osmosis (MF-RO) pilot plant. *Journal of Hazardous Materials*, *282*, 165–173. https://doi.org/10.1016/j.jhazmat.2014.09.015

Shainsky, N., Dobrynin, D., Ercan, U., Joshi, S. G., Ji, H., Brooks, A., Fridman, G., Cho, Y., Fridman, A., & Friedman, G. (2012). Plasma acid: Water treated by dielectric barrier discharge. *Plasma Processes and Polymers*, *9*, 1–6.

Vieno, N., Tuhkanen, T., & Kronberg, L. (2007). Elimination of pharmaceuticals in sewage treatment plants in Finland. *Water Research*, *41*, 1001–1012. https://doi.org/10.1016/j.watres.2006.12.017

Wanda, E. M., Nyoni, H., Mamba, B. B., & Msagati, T. A. (2017). Occurrence of emerging micropollutants in water systems in Gauteng, Mpumalanga, and North West Provinces, South Africa. *International Journal of Environmental Research and Public Health*, *14*, 79.

Wardenier, N. (2016). Nonequilibrium plasma in contact with water as advanced oxidation process for decomposition of micro pollutants.

Wardenier, N., Vanraes, P., Nikiforov, A., Van Hulle, S. W. H., & Leys, C. (2019). Removal of micropollutants from water in a continuous-flow electrical discharge reactor. *Journal of Hazardous Materials*, *362*, 238–245. https://doi.org/10.1016/j.jhazmat.2018.08.095

SUPPORTING INFORMATION

Additional supporting information can be found online in the Supporting Information section at the end of this article.

How to cite this article: Gwanzura, E., Ramjugernath, D., & Iwarere, S. A. (2023). Removal efficiency and energy consumption optimization for carbamazepine degradation in wastewater by electrohydraulic discharge. *Water Environment Research*, *95*(8), e10915. https://doi.org/10.1002/wer.10915